Anions Enhance Rare Earth Adsorption at Negatively Charged Surfaces

*Srikanth Nayak,[1] Kaitlin Lovering,[1] Wei Bu,[2] and Ahmet Uysal[1, *]*

[1]Chemical Sciences and Engineering Division, Argonne National Laboratory, Argonne IL 60439

[2]NSF's ChemMatCARS, The University of Chicago, Chicago IL 60637
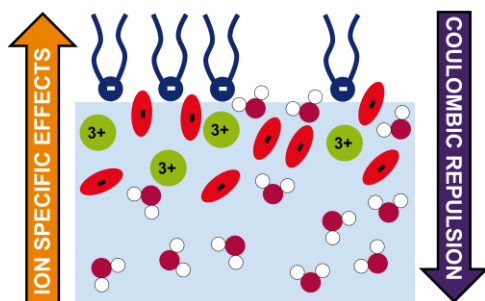
AUTHOR INFORMATION

Corresponding Author

*E-mail: ahmet@anl.gov. Web: www.anl.gov/profile/ahmet-uysal . Phone: +1-630-252-9133

ABSTRACT

Anions are expected to be repelled from negatively charged surfaces. At aqueous interfaces, however, ion-specific effects can dominate over direct electrostatic interactions. Using multiple *in situ* surface sensitive experimental techniques, we show that surface affinity of SCN^- ions are so strong that they can adsorb at a negatively charged floating monolayer at the air/aqueous interface. This extreme example of ion-specific effects may be very important for understanding complex processes at aqueous interfaces, such as chemical separations of rare earth metals. Adsorbed SCN^- ions at the floating monolayer increase the overall negative charge density, leading to enhanced trivalent rare earth adsorption. Surface sensitive X-ray fluorescence measurements show that the surface coverage of Lu^{3+} ions can be triple of the apparent surface charge of the floating monolayer in the presence of SCN^-. Comparison to NO_3^- samples show that the effects are strongly dependent to the character of the anion, providing further evidence to ion-specific effects dominating over electrostatics.

TOC GRAPHICS

KEYWORDS Ion-specific effects, overcharging, aqueous interfaces, vibrational spectroscopy

Ion adsorption and transfer at aqueous interfaces are very important in various processes, including atmospheric chemistry,[1] geochemistry,[2] biology,[3] energy storage,[4] and chemical separations.[5-6] It is reasonable to use classical double layer models, such as Gouy-Chapman, as a first approximation to describe the behavior of ions at aqueous interfaces. However, classical mean-field theories usually fail at high ionic strengths, when ion-ion and ion-solvent interactions start to dominate.[7] The ion concentration at interfaces can easily be orders of magnitude higher than the bulk, and interfacial water does not behave like a uniform dielectric background with a fixed dielectric constant. The dielectric constant drops to ~1 from ~80 within a few nanometers and interfacial water is structured.[2, 5, 8] Therefore, even at low bulk ion concentrations, especially with trivalent ions,[5, 9-10] ion-ion correlations may dominate and lead to phase transitions[5] and charge inversion.[11-13]

In aqueous solutions, the behavior of the ion depends on many more factors than its total charge. Broadly defined as ion-specific effects,[3, 14-15] the factors such as hydration enthalpy, charge distribution, and ionic radius, may be the dominant factors in determining the ion adsorption and transfer. Although ion-specific effects have been known since the famous experiments of Hofmeister,[3, 16] it is difficult to describe them with a unified, molecular-scale model, especially when the surface functionalization and ion-ion correlations originating from direct electrostatic interactions creates a complex network of interactions.[15-16] The recent advancements in surface specific spectroscopy[15, 17-21] and computational[22] methods, provide new opportunities in understanding these complex interfacial interactions.

Solvent extraction (SX), transfer of target ions from an aqueous phase into an organic phase with the help of amphiphilic extractants, provides interesting examples to ion-specific effects in high ionic strength conditions (Figure 1a).[23] In a typical SX process, aqueous phase may contain

highly concentrated background ions, such as NO_3^-, Cl^-, or SCN^- in addition to the metal ions that will be separated. When trivalent rare earth metals are the target ions, both direct electrostatic interactions and ion-specific effects become important. Rare earths are very similar chemically, and it is very difficult to separate them from each other.[24-25] The subtle differences between them, mostly originating from the lanthanide contraction,[26] is very important in their efficient separations. However, they have rarely been investigated from an ion-specific effect perspective.
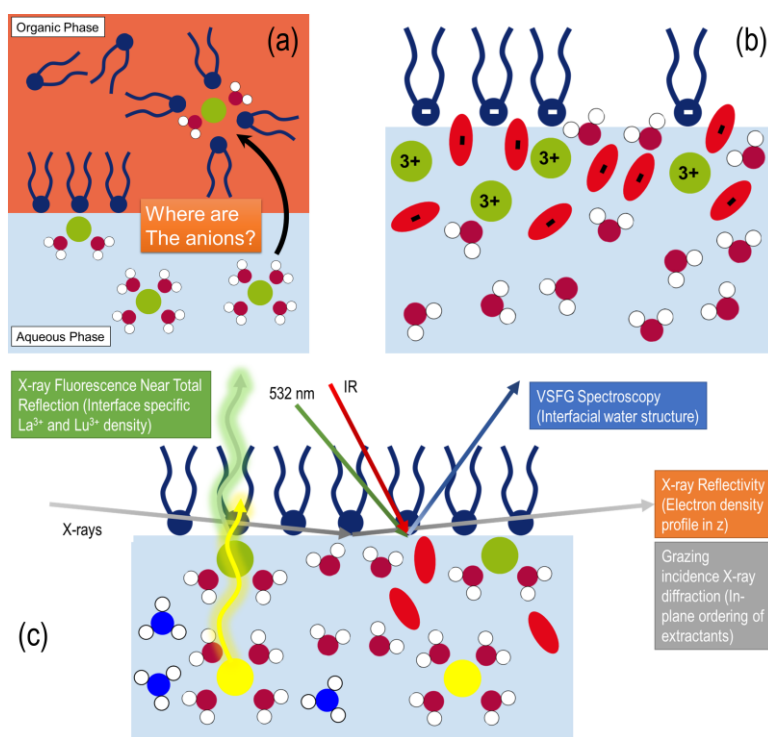

Figure 1. (a) A schematic representing the transfer of trivalent rare earth metals (green) from an aqueous phase with the assistance of amphiphilic extractants (blue). Although positively charged metal ions interact directly with the negatively charged extractants, and anions are expected to be repelled from the interface, the character of the anion may have significant effects on the extraction process. (b) A schematic representation of the main experiment presented in this Letter. SCN^- ions (red ellipses) are surface active, increasing Lu^{3+} (green) ion adsorption. (c) A schematic

explanation of XR, GID, XFNTR, and VSFG spectroscopy techniques used in this study to explore anion and rare earth adsorption at air/DHDP/aqueous interface. Blue, red, and white circles represent nitrogen, oxygen, and hydrogen, respectively. La^{3+} (yellow) and Lu^{3+} (green) ions emit X-ray fluorescence (represented by wiggly arrows) at distinct wavelengths allowing to quantify their surface coverage. A combination of these four techniques provide an opportunity to connect interfacial extractant, cation, anion, and water structures to obtain a detailed description of the interfacial processes.

Accessing the oil/aqueous interface during the actual extraction is very difficult. Therefore, model systems at oil/aqueous interface and air/aqueous interface, as well as computer simulations have been used to identify important aspects of ion adsorption, ion-extractant interactions, and ion transport in SX.[6, 17, 27-34] Surface specific X-ray reflectivity (XR),[6, 17, 27-30] neutron reflectivity (NR),[33] grazing incidence X-ray diffraction (GID),[5, 9, 28-29] X-ray fluorescence near total reflection (XFNTR),[17, 27, 29] vibrational sum frequency generation (VSFG) spectroscopy,[28, 31, 34] second harmonic generation (SHG) spectroscopy,[32] and molecular dynamics (MD) simulations[34-35] have been shown to be very useful in obtaining surface specific molecular scale information.

A recent XFNTR study showed that Er^{3+} ions are preferentially adsorbed at negatively charged monolayers of extractants from a mixture of Er^{3+} and Nd^{3+}, and the surface charge density showed a first order phase transition as a function of the bulk lanthanide concentration.[5] The preference of Er^{3+} over Nd^{3+} is in good agreement with the well-known preferential extraction of heavy lanthanides with acidic extractants. However, the study was done at very low ion concentrations, without any significant amount of background salts. It is known that the concentration and the character of the background anions are very important in determining the extraction efficiency of lanthanides when basic and neutral extractants are used.[23-24] Although it is reasonable to expect

minimal effects from anions when the extractant is acidic and directly coordinating the trivalent metal ion while repelling the anions electrostatically, here we show that non-Coulombic interactions cause non-negligible presence of anions at the interface under negatively charged monolayers.

In this Letter, we studied adsorption of Lu^{3+} (Z=71) and La^{3+} (Z=57) ions at floating dihexadecyl phosphate (DHDP) monolayers in the presence of 50 to 250 mM NO_3^- and SCN^- ions. We combined surface specific XR, XFNTR, GID, and VSFG techniques (Figure 1b) to identify the effects of background anions at the interfacial water structure and lanthanide adsorption. Our results show that anions play a significant role even at a negatively charged surface, where they are expected to be repelled by electrostatic interactions. The order of magnitude difference between the effects of NO_3^- and SCN^- on lanthanide adsorption show that non-Coulombic forces and interfacial water structure play significant roles in addition to the ion-ion correlations at the interface.
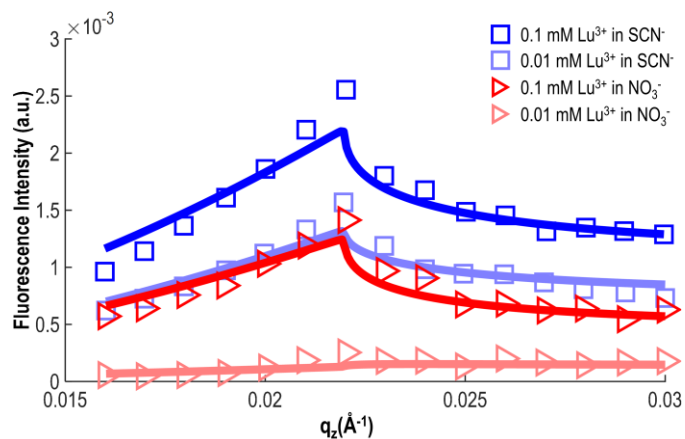

Figure 2. XFNTR data and fits (symbols and lines, respectively) of 0.01 mM Lu^{3+} (pink triangles) and 0.1 mM Lu^{3+} (red triangles) with 50 mM $NaNO_3$, pH 2.6 background and 0.01 mM Lu^{3+} (light blue squares) and 0.1 mM Lu^{3+} (blue squares) in 50 mM NaSCN, pH 2.6

background solutions. At both concentrations, more Lu^{3+} cations are adsorbed in the presence of thiocyanate (squares) than nitrate (triangles).

Figure 2 shows XFNTR data for Lu^{3+} adsorption at DHDP monolayer in the presence of 50 mM NO_3^- or SCN^- as a function of anion type and bulk Lu^{3+} concentration based. In this experiment, the fluorescence signal from Lu^{3+} ions are measured by an energy dispersive detector 10 mm above the surface, as a function of the incidence angle, α, where $q_z = \frac{4\pi}{\lambda} \sin\left(\frac{2\alpha}{2}\right)$ and λ=0.73 Å. Below critical angle ($\alpha < \alpha_c = 0.022$ Å^{-1}), X-rays go under total external reflection and therefore, only the Lu^{3+} ions within the few nanometers of the surface fluoresce (Figure 1b).[17, 27] The linearly increasing signal, as a function of q_z, below the critical angle is a signature of excess ion adsorption at the interface. To fit the data (Figure 2, solid lines), we used a model, considering the X-ray absorption and emission energies, illuminated volume based on the beam size, and the detector size and distance (Supporting Information).[27]

Lu^{3+} adsorbs significantly better in SCN^- background than it does in NO_3^- background. The bulk Lu^{3+} concentration also affects the adsorbed ion density. When the bulk Lu^{3+} concentration is 0.01 mM, unit area per Lu^{3+} is 877 ± 33 Å^2 and 84 ± 5 Å^2 in NO_3^- and SCN^- backgrounds, respectively. This corresponds to an order of magnitude more surface density by just changing the type of the anion in the background solution. When we increase the bulk Lu^{3+} concentration to 0.1 mM, the unit area per Lu^{3+} becomes 95 ± 3 Å^2 in NO_3^- and 52 ± 2 Å^2 in SCN^- solutions.

Considering that the molecular area for DHDP (p$K_a = 2.1$) is 40.5 Å^2 (Figure S2b) and 76% of them are negatively charged at pH = 2.6,[36] the surface density of Lu^{3+} in SCN^- background and 0.1 mM bulk Lu^{3+} concentration corresponds to 1 Lu^{3+} per 1 DHDP$^-$ which requires 2 SCN^- molecules per Lu^{3+} at the interface for charge balance. Even at the lower bulk concentration of 0.01 mM, Lu^{3+} ions apparently overcompensate the surface charge of the monolayer, which requires 1.2

SCN$^-$ molecules per Lu^{3+} for charge balance. These results are in stark contrast to the adsorption behavior observed in a previous study, without any excess anion in the background, where the maximum lanthanide adsorption was limited by the surface charge of the monolayer (1 lanthanide per 3 ODPA$^-$, octadecylphosphonic acid, molecule).[9]

Some assumptions may affect the calculations above. First, although 24% of DHDP molecules are expected to be protonated based on pK$_a$ value, Lu^{3+} ions may be replacing those protons. In a similar consideration, bulk salt concentration is known to affect the monolayer protonation state.[37] These affects may lead to slightly smaller Lu^{3+}/DHDP$^-$ ratios than we calculated. Though it would not change the overall trends and conclusions. Also, there are few mM Cl$^-$ ions from the LuCl$_3$ salt and pH adjustment with HCl, and 250 mM Na$^+$ from NaSCN or NaNO$_3$ salts in the solution. Cl$^-$ ions are not surface active in general and their bulk concentration is very small to make any effect. Na$^+$ ions are also not surface active, but they will still be competing with Lu^{3+}, due to their high bulk concentration. Nevertheless, our experiments compare NaSCN to NaNO$_3$ salts and focus on the differences between them, allowing us to identify the effects of SCN$^-$ and NO$_3^-$.

It is reasonable to ask if SCN$^-$ can really adsorb to the negatively charged surface. Because, it is also possible that Lu^{3+} ions overcompensate the surface charge of the monolayer and attract SCN$^-$ ions to the surface.[11] To find the answer to this question, we conducted XR and VSFG measurements of DHDP monolayers on SCN$^-$ and NO$_3^-$ solutions without any lanthanides in the solution. Both experiments indicate that SCN$^-$ ions adsorb at the interface even without the lanthanides.
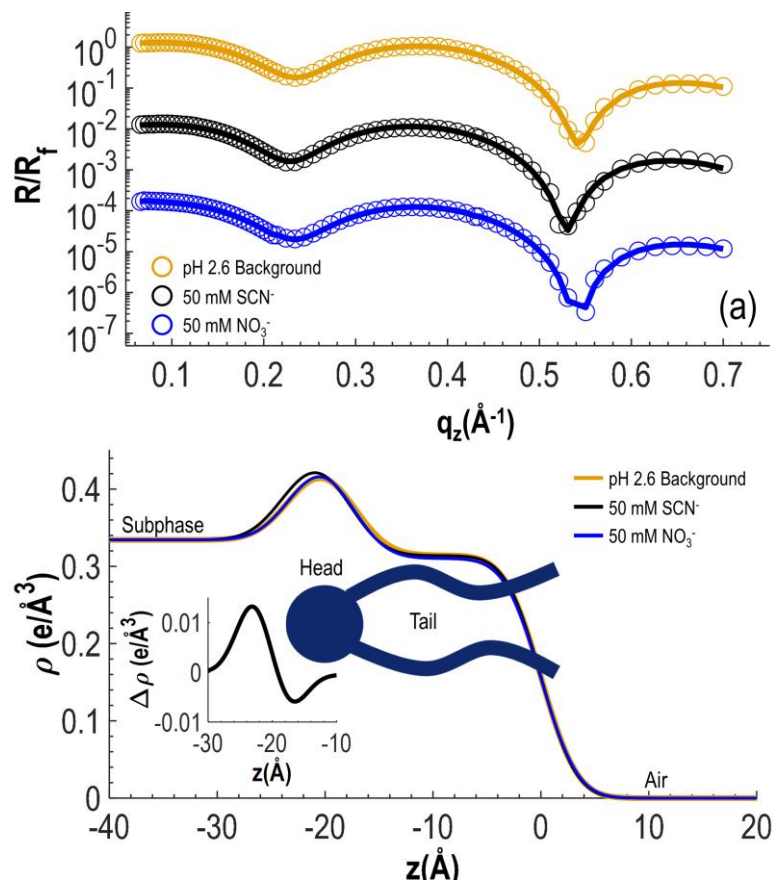
Figure 3. (a) Fresnel normalized XR data (symbols) and fits (solid lines) of DHDP monolayers at air/aqueous interface. The pH 2.6 (yellow) and $NaNO_3$ (blue) data look almost identical, while the second minimum of NaSCN data (black) is shifted to lower q_z. (b) EDPs derived from the fits in (a) with the same color codes. Inflection points of the tail groups are assigned as $z = 0$. The $NaNO_3$ structure (blue) is almost identical with the background (yellow). NaSCN headgroup region has slightly higher electron density and thickness. The inset shows the differential EDP, calculated by subtracting pH 2.6 (yellow) from NaSCN (black).

Figure 3a shows the XR data (symbols) and the fit (lines) of DHDP monolayers on pH 2.6 water, 50 mM SCN⁻, and 50 mM NO₃⁻ solutions. 50 mM NO₃⁻ (blue symbols) data is almost identical to the one obtained on pH 2.6 background solution. The minima of XR data from 50 mM SCN⁻ (black symbols) shifted toward lower q_z, suggesting a thicker interfacial region. We can determine the

interfacial electron density profile (EDP) by fitting the XR data using a 2-layer model. One layer corresponds to the tail group of the DHDP molecules and the other layer represents the headgroup and adsorbed ion region. The XR signal from this model interface was calculated by using Parratt formalism.[17, 38] The thickness, electron density, and interfacial roughness (represented by error functions) of the layers were determined from the least square fitting of the calculated curves to the experimental data (Figure 3a, solid lines). The resulting EDPs are shown in Figure 3b. While the NO_3^- sample is identical to the background, headgroup region of SCN^- sample is slightly thicker and denser.

We subtracted the background EDP (yellow) from SCN^- EDP (black) to quantify the SCN^- coverage (Figure 3b, inset). The area under the differential EDP is 1.3 e^- / $Å^2$. Considering that SCN^- has 30 electrons, we determine that the molecular area for SCN^- ions is ~24 $Å^2$. This is a very rough calculation and probably an underestimate. Because, it is possible that SCN^- ions push water molecules from the interface,[28] also XR cannot detect less organized ions in the diffuse layer, since they do not create a significant electron density gradient.[29] Our approximation does not take these into account. Nevertheless, 1 SCN^- in 24 $Å^2$ is very close to 2 SCN^- per 1 $DHDP^-$ ratio expected from the charge balance of Lu^{3+} adsorption.

Figure 4 shows OH region of the VSFG data of DHDP monolayers on 50 mM and 250 mM NO_3^- and SCN^- solutions. A comparison of 50 mM NO_3^- and SCN^- data (light blue triangles and gray squares, respectively) show that while the signal from NO_3^- solution keeps its bimodal character, the signal from SCN^- solution becomes a single red-shifted peak. Interestingly, this adsorption trend is very similar to the one observed under positively charged DPTAP (1,2-Dipalmitoyl-3-trimethylammonium-propane) monolayers,[28] except it happens at a much higher bulk SCN^- concentration. As the bulk concentration increased to 250 mM, VSFG signals are almost

indistinguishable from the background. However, it is possible to claim the existence of a small signal in NO_3^- system.
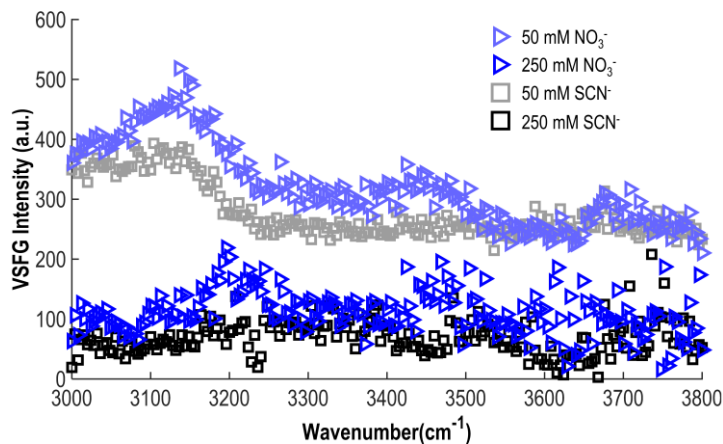

Figure 4. SFG Spectra of DHDP/aqueous interfaces with 50 and 250 mM solutions of $NaNO_3$ (light and dark blue triangles) and NaSCN (gray and black squares). 50 mM data is shifted by +200 for clarity. Although Na^+ ions are mainly expected to interact with the negatively charged DHDP monolayer, the spectra show clear differences based on the anion character.

The VSFG spectra of air/aqueous interface, under various conditions, have been reported in the literature.[20, 28, 34, 39-41] It is possible to identify a bimodal water signal around 3000-3500 cm^{-1} due to the orientational ordering of water molecules at bare air/water the interface. Presence of charged monolayers, such as DHDP, creates a fixed electric field and the resulting interfacial ordering increases the VSFG signal, usually known as $\chi^{(3)}$ effect.[41-44] Adsorbed ions at the interface typically disturb the orientational ordering of water molecules and shield the electric field, leading to a decrease in the interfacial water signal. It is very common to utilize this signal decrease in order to probe the surface affinity of ions in the context of specific ion effects at positively charged interfaces.[45-46] For DHDP$^-$, Na^+ ions would be expected to adsorb and affect the surface structure from an electrostatic point of view. However, it is well-known that monovalent cations, especially

strongly hydrated Li^{+} and Na^{+} do not affect the interfacial structure significantly.[47] Nevertheless, some decrease in VSFG signal is expected, due to the electrostatic shielding of Na^{+} and the decrease in the $\chi^{(3)}$ effect. The effects observed for SCN[-] in the data in Figure 4 is significantly beyond that expected interaction.

SCN[-] behaves very differently compared to NO$_3$[-] and other halides at positively charged surfaces.[28] The current data in Figure 4, strongly suggests that the way SCN[-] ions affect the orientational water ordering is very similar under positively and negatively charged monolayers, observed as a red-shifted and narrowed VSFG signal, in good agreement with the overall observation of that the non-Coulombic forces are very dominant in SCN[-] adsorption.

When these results are considered together with the XR results presented in Figure 3, they demonstrate that the hydration and anion environment around the DHDP headgroups are significantly different in NO$_3$[-] and SCN[-] solutions. SCN[-] ions are visible in XR data and have significant effects on interfacial water structure. However, NO$_3$[-] ions cannot be detected by XR and their effects on the interfacial water structure cannot be distinguished from a typical $\chi^{(3)}$ effect.

A comparison of La^{3+} vs Lu[3+] adsorption in SCN[-] and NO$_3$[-] media provide further information about adsorption pathways of lanthanides and the effects of the anions. The presence of excess anions does not change the preference of heavy lanthanides over the light ones. XFNTR studies show significantly less La^{3+} (Z=57) coverage (200 ± 5 Å^2 / ion) at the interface compared to Lu[3+] (Z=71) coverage (95 ± 3 Å^2 / ion) (Figure S1a), similar to previous observations.[5] Even very small La^{3+} adsorption in NO$_3$[-] system almost diminishes all VSFG signal (Figure S1b). The relative effect of La^{3+} adsorption on VSFG signal in SCN[-] medium is smaller (Figure S2a). We interpret this difference as SCN[-] ions had changed the interfacial water structure significantly and small amount of La^{3+} adsorption has minimal effect on this new structure. In contrast, NO$_3$[-] ions are

known to fit into existing hydrogen bonding network of water molecules, without effecting the VSFG signal significantly, even at positively charged surfaces.[28] Therefore, even a small amount of La^{3+} adsorption lead to very dramatic changes in VSFG signal (Figure S1b). These subtle differences are only visible in La^{3+} systems. Lu^{3+} adsorbs very strongly in all conditions we studied and diminish all VSFG signal from hydrogen-bonded water region completely. At the 84 ± 5 $Å^2$ ionic area (Figure S2a, blue squares), in SCN^- free-OH peak becomes visible, a signature of disturbance of the monolayer due to adsorbed ions,[28] allowing some water molecules to stick out of the interface. The decreased domain size of the monolayer film observed in GID experiments also confirm this interpretation (Figure S2b).

All the experiments were done at acidic conditions (pH = 2.6) to avoid hydrolysis and formation of species other than simple trivalent lanthanide ions. It is known that multivalent ions can form larger oligomers and even nanoparticles in aqueous solutions which can have significant effects on surface adsorption.[48]

The interactions of amphiphiles with trivalent ions at an aqueous interface is a key step in many industrially and scientifically important processes, especially in chemical separations.[17, 22-23, 28, 35] It is known that small differences between trivalent lanthanides make it possible to separate them from each other by using solvent extraction.[23-24, 26] However, the molecular scale details of the process, especially in high ionic strength conditions, which are typical in SX, are underexplored. In this work, we investigated an extreme example of ion-specific effects, where SCN^- ions are adsorbed at a negatively charged surface and triple the amount of rare earth adsorption at this interface. We showed that without any lanthanides in the subphase SCN^- ions can adsorb at the negatively charged surface and their effect to the interfacial electron density can be detected by XR. VSFG experiments under same conditions show a significant change in the interfacial water

structure with SCN$^-$ adsorption. The disappearance of higher frequency part of the hydrogen bonded water signal is very similar to the effect observed under positively charged monolayers,[28] suggesting that the adsorption pathway of SCN$^-$ is mainly dictated by non-Coulombic effects. The effects of NO$_3^-$ to interfacial EDP is below the detection limits of XR and its effects on VSFG signal is much smaller.

The presence of anions did not change the trend about preferential adsorption of heavier Lu^{3+} over lighter La^{3+}. However, the character of the anion significantly affected the amount of the adsorption. SCN$^-$ anions lead to much higher adsorption of Lu^{3+} ions. These results provide a detailed picture of interfacial ion adsorption and water structures by integrating multiple methods sensitive to different components present at the interface and clearly demonstrating the interplay between Coulombic and non-Coulombic forces. These model experiments will be an important step in understanding the ion-ion, ion-amphiphile, and ion-solvent interactions in complex fluids and at functionalized surfaces.

ASSOCIATED CONTENT

Supporting Information. The following files are available free of charge.

Experimental details; additional XFNTR, VSFG, and GID data; XR fit parameters. (PDF)

AUTHOR INFORMATION

Corresponding Author

*E-mail: ahmet@anl.gov. Web: www.anl.gov/profile/ahmet-uysal . Phone: +1-630-252-9133

Notes

The authors declare no competing financial interests.

REFERENCES

1.   Baumler, S. M.; Allen, H. C. Vibrational Spectroscopy of Gas–Liquid Interfaces. In *Physical Chemistry of Gas-Liquid Interfaces*, Faust, J. A.; House, J. E., Eds. Elsevier: 2018; pp 105-133.

2.   Fenter, P.; Lee, S. S. Hydration layer structure at solid-water interfaces. *Mrs. Bull.* **2014,** *39* (12), 1056-1061.

3.   Lo Nostro, P.; Ninham, B. W. Hofmeister phenomena: an update on ion specificity in biology. *Chem. Rev.* **2012,** *112* (4), 2286-322.

4.   Merlet, C. l.; Péan, C.; Rotenberg, B.; Madden, P. A.; Simon, P.; Salanne, M. Simulating Supercapacitors: Can We Model Electrodes As Constant Charge Surfaces? *J. Phys. Chem. Lett.* **2012,** *4* (2), 264-268.

5.   Miller, M.; Liang, Y.; Li, H.; Chu, M.; Yoo, S.; Bu, W.; Olvera de la Cruz, M.; Dutta, P. Electrostatic Origin of Element Selectivity during Rare Earth Adsorption. *Phys. Rev. Lett.* **2019,** *122* (5), 058001.

6.   Liang, Z.; Bu, W.; Schweighofer, K. J.; Walwark, D. J., Jr.; Harvey, J. S.; Hanlon, G. R.; Amoanu, D.; Erol, C.; Benjamin, I.; Schlossman, M. L. Nanoscale view of assisted ion transport across the liquid-liquid interface. *Proc. Natl. Acad. Sci. U. S. A.* **2019,** *116* (37), 18227-18232.

7.   Smith, A. M.; Lee, A. A.; Perkin, S. The Electrostatic Screening Length in Concentrated Electrolytes Increases with Concentration. *J. Phys. Chem. Lett.* **2016,** *7* (12), 2157-63.

8.   Luo, G. M.; Bu, W.; Mihaylov, M.; Kuzmenko, I.; Schlossman, M. L.; Soderholm, L. X-ray Reflectivity Reveals a Nonmonotonic Ion-Density Profile Perpendicular to the Surface of ErCl3 Aqueous Solutions. *J. Phys. Chem. C* **2013,** *117* (37), 19082-19090.

9.   Miller, M.; Chu, M.; Lin, B.; Bu, W.; Dutta, P. Atomic Number Dependent "Structural Transitions" in Ordered Lanthanide Monolayers: Role of the Hydration Shell. *Langmuir* **2017,** *33* (6), 1412-1418.

10.   Lee, S. S.; Schmidt, M.; Laanait, N.; Sturchio, N. C.; Fenter, P. Investigation of Structure, Adsorption Free Energy, and Overcharging Behavior of Trivalent Yttrium Adsorbed at the Muscovite (001)-Water Interface. *J. Phys. Chem. C* **2013,** *117* (45), 23738-23749.

11.   Pittler, J.; Bu, W.; Vaknin, D.; Travesset, A.; McGillivray, D. J.; Loesche, M. Charge inversion at minute electrolyte concentrations. *Phys. Rev. Lett.* **2006,** *97* (4), 046102.

12.   Miller, M.; Chu, M.; Lin, B.; Meron, M.; Dutta, P. Observation of Ordered Structures in Counterion Layers near Wet Charged Surfaces: A Potential Mechanism for Charge Inversion. *Langmuir* **2016,** *32* (1), 73-7.

13.   Roosen-Runge, F.; Heck, B. S.; Zhang, F.; Kohlbacher, O.; Schreiber, F. Interplay of pH and Binding of Multivalent Metal Ions: Charge Inversion and Reentrant Condensation in Protein Solutions. *J. Phys. Chem. B* **2013,** *117* (18), 5777-5787.

14.   Mazzini, V.; Craig, V. S. J. What is the fundamental ion-specific series for anions and cations? Ion specificity in standard partial molar volumes of electrolytes and electrostriction in water and non-aqueous solvents. *Chem. Sci.* **2017,** *8* (10), 7052-7065.

15.   Leontidis, E. Investigations of the Hofmeister series and other specific ion effects using lipid model systems. *Adv. Colloid. Interfac.* **2017,** *243*, 8-22.

16.   Jungwirth, P.; Cremer, P. S. Beyond Hofmeister. *Nat. Chem.* **2014,** *6* (4), 261-3.

17.   Bera, M. K.; Bu, W.; Uysal, A. Liquid Surface X-Ray Scattering. In *Physical Chemistry of Gas-Liquid Interfaces*, Faust, J. A.; House, J. E., Eds. Elsevier: 2018; pp 167-194.

18.   Backus, E. H. G.; Bonn, M.; Nagata, Y. Molecular Structure and Dynamics of Water at the Water-Air Interface Studied with Surface-Specific Vibrational Spectroscopy. *Angew. Chem. Int. Ed.* **2015,** *54* (19), 5560-5576.

19.   Zdrali, E.; Okur, H. I.; Roke, S. Specific Ion Effects at the Interface of Nanometer-Sized Droplets in Water: Structure and Stability. *J. Phys. Chem. C* **2019,** *123* (27), 16621-16630.

20.   Johnson, C. M.; Baldelli, S. Vibrational sum frequency spectroscopy studies of the influence of solutes and phospholipids at vapor/water interfaces relevant to biological and environmental systems. *Chem. Rev.* **2014,** *114* (17), 8416-46.

21.   Azam, M. S.; Weeraman, C. N.; Gibbs-Davis, J. M. Specific Cation Effects on the Bimodal Acid–Base Behavior of the Silica/Water Interface. *J. Phys. Chem. Lett.* **2012,** *3* (10), 1269-1274.

22.   Sun, P.; Huang, K.; Liu, H. Specific Salt Effect on the Interaction between Rare Earth Ions and Trioctylphosphine Oxide Molecules at the Organic-Aqueous Two-Phase Interface: Experiments and Molecular Dynamics Simulations. *Langmuir* **2018,** *34* (38), 11374-11383.

23.   Nayak, S.; Lovering, K.; Uysal, A. Ion-Specific Clustering of Metal-Amphiphile Complexes in Rare Earth Separations. *ChemRxiv. Preprint.* **2020,** 10.26434/chemrxiv.11938182.v1.

24.   Baldwin, A. G.; Ivanov, A. S.; Williams, N. J.; Ellis, R. J.; Moyer, B. A.; Bryantsev, V. S.; Shafer, J. C. Outer-Sphere Water Clusters Tune the Lanthanide Selectivity of Diglycolamides. *ACS Cent. Sci.* **2018,** *4* (6), 739-747.

25.   Sholl, D. S.; Lively, R. P. Seven chemical separations to change the world. *Nature* **2016,** *532* (7600), 435-7.

26.   Ferru, G.; Reinhart, B.; Bera, M. K.; Olvera de la Cruz, M.; Qiao, B.; Ellis, R. J. The Lanthanide Contraction beyond Coordination Chemistry. *Chem. Eur. J.* **2016,** *22* (20), 6899-904.

27.   Bu, W.; Mihaylov, M.; Amoanu, D.; Lin, B.; Meron, M.; Kuzmenko, I.; Soderholm, L.; Schlossman, M. L. X-ray studies of interfacial strontium-extractant complexes in a model solvent extraction system. *J. Phys. Chem. B* **2014,** *118* (43), 12486-500.

28.   Lovering, K.; Nayak, S.; Bu, W.; Uysal, A. The Role of Specific Ion Effects in Ion Transport: The Case of Nitrate and Thiocyanate. *J. Phys. Chem. C* **2020,** *124* (1), 573-581.

29.   Uysal, A.; Rock, W.; Qiao, B. F.; Bu, W.; Lin, B. H. Two-Step Adsorption of PtCl62- Complexes at a Charged Langmuir Monolayer: Role of Hydration and Ion Correlations. *J. Phys. Chem. C* **2017,** *121* (45), 25377-25383.

30.   Rock, W.; Oruc, M. E.; Ellis, R. J.; Uysal, A. Molecular Scale Description of Anion Competition on Amine-Functionalized Surfaces. *Langmuir* **2016,** *32* (44), 11532-11539.

31.   Chowdhury, A. U.; Lin, L.; Doughty, B. Hydrogen-Bond Driven Chemical Separations: Elucidating the Inter-facial Steps of Self-Assembly in Solvent Extraction. *ChemRxiv. Preprint.* **2020**, 10.26434/chemrxiv.11926860.v1.

32.   Gassin, P. M.; Martin-Gassin, G.; Meyer, D.; Dufreche, J. F.; Diat, O. Kinetics of Triton-X100 Transfer Across the Water/Dodecane Interface: Analysis of the Interfacial Tension Variation. *J. Phys. Chem. C* **2012,** *116* (24), 13152-13160.

33.   Scoppola, E.; Watkins, E. B.; Campbell, R. A.; Konovalov, O.; Girard, L.; Dufreche, J. F.; Ferru, G.; Fragneto, G.; Diat, O. Solvent Extraction: Structure of the Liquid-Liquid Interface Containing a Diamide Ligand. *Angew. Chem. Int. Edit.* **2016,** *55* (32), 9326-30.

34.   Rock, W.; Qiao, B. F.; Zhou, T. C.; Clark, A. E.; Uysal, A. Heavy Anionic Complex Creates a Unique Water Structure at a Soft Charged Interface. *J. Phys. Chem. C* **2018,** *122* (51), 29228-29236.

35.   Servis, M. J.; Clark, A. E. Surfactant-enhanced heterogeneity of the aqueous interface drives water extraction into organic solvents. *Phys. Chem. Chem. Phys.* **2019,** *21* (6), 2866-2874.

36.   Wang, W.; Park, R. Y.; Meyer, D. H.; Travesset, A.; Vaknin, D. Ionic specificity in pH regulated charged interfaces: Fe3+ versus La3+. *Langmuir* **2011,** *27* (19), 11917-24.

37.   Sung, W.; Avazbaeva, Z.; Kim, D. Salt Promotes Protonation of Amine Groups at Air/Water Interface. *J. Phys. Chem. Lett.* **2017,** *8* (15), 3601-3606.

38.   Danauskas, S. M.; Li, D. X.; Meron, M.; Lin, B. H.; Lee, K. Y. C. Stochastic fitting of specular X-ray reflectivity data using StochFit. *J. Appl. Cryst.* **2008,** *41* (6), 1187-1193.

39.   Bonn, M.; Nagata, Y.; Backus, E. H. Molecular structure and dynamics of water at the water-air interface studied with surface-specific vibrational spectroscopy. *Angew. Chem. Int. Edit.* **2015,** *54* (19), 5560-76.

40.   Ma, G.; Chen, X.; Allen, H. C. Dangling OD confined in a Langmuir monolayer. *J. Am. Chem. Soc.* **2007,** *129* (45), 14053-7.

41.   Wen, Y. C.; Zha, S.; Liu, X.; Yang, S.; Guo, P.; Shi, G.; Fang, H.; Shen, Y. R.; Tian, C. Unveiling Microscopic Structures of Charged Water Interfaces by Surface-Specific Vibrational Spectroscopy. *Phys. Rev. Lett.* **2016,** *116* (1), 016101.

42.   Joutsuka, T.; Morita, A. Electrolyte and Temperature Effects on Third-Order Susceptibility in Sum-Frequency Generation Spectroscopy of Aqueous Salt Solutions. *J. Phys. Chem. C* **2018,** *122* (21), 11407-11413.

43.   Schaefer, J.; Gonella, G.; Bonn, M.; Backus, E. H. G. Surface-specific vibrational spectroscopy of the water/silica interface: screening and interference. *Phys. Chem. Chem. Phys.* **2017,** *19* (25), 16875-16880.

44.   Ohno, P. E.; Wang, H. F.; Geiger, F. M. Second-order spectral lineshapes from charged interfaces. *Nat. Commun.* **2017,** *8* (1), 1032.

45.   Nihonyanagi, S.; Yamaguchi, S.; Tahara, T. Counterion effect on interfacial water at charged interfaces and its relevance to the Hofmeister series. *J. Am. Chem. Soc.* **2014,** *136* (17), 6155-8.

46.   Sung, W.; Wang, W.; Lee, J.; Vaknin, D.; Kim, D. Specificity and Variation of Length Scale over Which Monovalent Halide Ions Neutralize a Charged Interface. *J. Phys. Chem. C* **2015,** *119* (13), 7130-7137.

47.   Okur, H. I.; Kherb, J.; Cremer, P. S. Cations Bind Only Weakly to Amides in Aqueous Solutions. *J. Am. Chem. Soc.* **2013,** *135* (13), 5062-5067.

48.   Yuan, K.; Bracco, J. N.; Schmidt, M.; Soderholm, L.; Fenter, P.; Lee, S. S. Effect of Anions on the Changes in the Structure and Adsorption Mechanism of Zirconium Species at the Muscovite (001)–Water Interface. *J. Phys. Chem. C* **2019,** *123* (27), 16699-16710.